Enterobacter Mucoid Conversion Blocks Coaggregation with Aeromonas

by

BAILEY R. BARRETT

A THESIS

Presented to the Department of Biology
and the Robert D. Clark Honors College
in partial fulfillment of the requirements for the degree of
Bachelor of Science

May 2024

An Abstract of the Thesis of

Bailey Barrett for the degree of Bachelor of Science
in the Department of Biology to be taken May 2024

Title: *Enterobacter* Mucoid Conversion Blocks Coaggregation with *Aeromonas*

Approved: *Karen Guillemin, Ph.D.*
Primary Thesis Advisor

The vertebrate gut is a dynamic environment, harboring diverse bacteria that interact with both each other and their host. These interactions can profoundly influence host health, shaping host traits such as development and immunological functions across vertebrates--from zebrafish to humans. Despite its importance, the molecular basis of how microbes interact with each other is still poorly understood. Coaggregation, where genetically diverse microorganisms physically interact with one another to form multi-species clusters, is one type of interaction between microbes that can influence the spatial organization and physiology of microbial communities. Here, I provide mechanistic insights into genetic pathways that shape physical interactions between bacteria that reside in the vertebrate gut and determine how they shape the physiology of other community members.

My studies focused on identifying the molecular mechanisms facilitating coaggregation between two bacteria that coaggregate in the intestine of their host. I used the model bacterial species *Aeromonas* sp. ZOR0001 (Aer01) and *Enterobacter* sp. ZOR0014 (Ent14), which form dense coaggregates in the larval zebrafish gut. These bacteria provide an excellent model for studying microbial coaggregation because they are easy to culture outside the zebrafish, are genetically tractable, and coaggregate in culture conditions developed by the Guillemin lab.

To probe this interaction, I sought to identify the genetic pathways involved in coaggregation for both organisms. First, I leveraged an existing mutant library of Aer01 with aggregation defects in our culture conditions and identified an Aer01 adhesin called MbpA that is necessary for binding Ent14. Using experimental evolution, I generated Ent14 mutants with deficits in coaggregating with Aer01, to identify potential cell surface factors on Ent14 recognized by MbpA. These evolved isolates form large, mucoid colonies, a phenotype that arose rapidly during experimental evolution. Genome analysis of two mucoid isolates revealed these isolates contain different mutations in the Regulator of Colanic Acid Synthesis (Rcs) system. Rcs-mediated upregulation of colanic acid polysaccharide (CAP) production is known to cause mucoidy. Production of this thick polysaccharide capsule can shield indispensable outer membrane factors targeted by host immune system as well as viruses that infect bacteria called bacteriophage. I show my evolved mucoid Ent14 isolates are hyperactive Rcs mutants, suggesting that rather than losing the cell surface factor recognized by MbpA, these mutants shield it from MbpA recognition. Further, I show that Ent14 mucoidy influences the physiology of microbes other than Aer01 that interact with Ent14. Together these data indicate the mucoid phenotype observed in the evolved Ent14 isolates not only alters their interaction with Aer01 but also has broader implications for microbial interactions and community dynamics. My research demonstrates the complex interplay between genetic pathways, phenotypic traits, and ecological consequences within microbial communities.

Acknowledgements

First and foremost, I would like to express my deepest gratitude to my mentors, Dr. Karen Guillemin and Dr. Jarrod Smith, whose guidance and support have been instrumental in the completion of this thesis.

Karen, I am profoundly thankful for having the opportunity to join your lab. Your willingness to accept me into your research group was a pivotal moment in my academic journey. The environment you have cultivated within your lab has allowed me to explore, learn, and grow both as a researcher and an individual. Your support, insightful advice, and teaching have been invaluable to me. Thank you very much for all of the time you have dedicated to me and my learning.

Jarrod, I am equally indebted to you for your mentorship and support. Your expertise and dedication have made my research experience the most incredible time I have spent at the University of Oregon. I deeply appreciate the time you have invested in guiding me through complex concepts and the thoughtful advice you have provided. Your encouragement and guidance have made my thesis project a great experience.

To both Dr. Guillemin and Dr. Smith, thank you for believing in my potential and for fostering an environment where I could thrive. Your combined mentorship has not only helped me achieve my academic goals but has also inspired me to pursue greater things in all my future endeavors. I am forever grateful for your contributions to my growth as a researcher and for the lasting impact you have made on my academic and personal development.

Table of Contents

Introduction

Multi-species Coaggregates are a Hallmark of Intestinal Health.

Elie Metchnikoff's pioneering Nobel Prize-winning work in 1908, showing the positive influence of microbes in yogurt on mammalian health, ushered in a new era of microbiological studies centered on the benefits of microbes to human well-being (Metchnikoff, 1908). Today, propelled by advancements in techniques and model systems, the field of microbiome research has expanded exponentially, with much research focused on the role of gut microbes in vertebrate intestinal health. However, despite significant advancements in research, we still have a poor understanding of the molecular processes leading to the assembly and localization of beneficial microbial communities in the gut and the role these processes have on host health.

Cross sections from healthy vertebrate intestines, including zebrafish, mouse, and human, show the microbes in the intestinal environment are clustered together in numerous multi-species communities called coaggregates in the gut lumen and mucosa (Bates, 2006; Fung, 2014). Changes to the spatial organization of bacteria in the gut have dramatic effects on intestinal health. While much attention has been paid to host factors that influence microbial behaviors and coaggregation, such as immune pathways and the production of glycan-rich mucus, little is known about the microbial factors that facilitate coaggregation or how microbially produced glycan-rich substrates such as exopolysaccharides or capsule, impact the physiology of neighboring microbes.

The Role of Coaggregation in Gut Microbiome Assembly and Host Interactions

Dysbiosis refers to the imbalance or disruption of the symbiotic relationship between microbial communities and their host organism. This imbalance can result from internal ecological factors, including changes in microbial composition, disruptions in community interactions, or alterations in the production of microbial metabolites (Levy, 2017). These disruptions have been implicated in the progression of numerous diseases, including inflammatory bowel disease, obesity, metabolic disorders, allergies, and even cardiovascular disease (Kennedy, 2014; Breton, 2022; Banyavanich, 2019; Novakovic, 2020) A major gap in our current understanding is how the crosstalk between microbial physiological traits and signaling pathways in complex communities influences the assembly of multi-species aggregates commonly observed in healthy guts.

Bacteria alter their cell-surface properties, metabolism, and production of virulence factors depending on their physiological state. Thus, health-promoting interactions with the host or other resident microbes are influenced by whether they exist as part of an aggregate or as free-floating entities. For example, the larval zebrafish resident microbe *Aeromonas* sp. ZOR0001 (Aer01) typically aggregates in the larval zebrafish gut and mutants that are unable to sense an abundant sugar found in this environment, N-acetylglucosamine (GlcNAc), no longer aggregate, are pro-inflammatory, and dramatically alter the community composition of a synthetic larval zebrafish microbial community (Smith, 2023; Sundarraman, 2022). Thus, uncovering the genetic determinants and ecological factors influencing coaggregation is crucial for furthering our understanding of gut microbiota dynamics and their implications in microbial physiology and host health.

Coaggregation and Interactions Among Zebrafish Microbes

In the larval zebrafish gut, *Aeromonas* sp. ZOR0001 (Aer01) forms tight coaggregates with another larval zebrafish resident microbe *Enterobacter* sp. ZOR0014 (Ent14). Previous work in the Guillemin lab has shown a highly motile Aer01 mutant, called MB4, that is unable to sense GlcNac, doesn't coaggregate with Ent14 and rapidly disaggregates aggregated Ent14, displacing it from the larval zebrafish gut (Sundarraman 2022). In a 5-member synthetic community of larval zebrafish isolates, MB4 also displaces the other members *Pseudomonas* sp. ZWU0006 (Pse06), *Acinetobacter* sp. ZOR0008 (Ac08), and *Plesiomonas* sp. ZOR0011 (Ple11). Here, Ent14 is still disaggregated by MB4, indicating the community structure and composition is dramatically impacted when the physiology of a single community member is altered. While these studies indicate Aer01 aggregation is critical for Aer01-Ent14 coaggregation, the genes involved in this interaction are not known.

A major goal of my thesis research is to identify Aer01 and Ent14 genes necessary for coaggregation between these two microbes. I will use previously characterized Aer01 mutants with aggregation defects to identify Aer01 factors and use experimental evolution to generate Ent14 mutants with defects in coaggregation with Aer01 to identify Ent14 factors. I will also determine how genetic pathways necessary for Ent14 interactions with Aer01 impact interactions with other community members, namely Pse06, Ac08, and Ple11. By understanding the genetic machinery driving bacterial coaggregation and spatial organization, I aim to uncover fundamental principles governing gut microbiome ecology. Insights gained from this study may inform future research endeavors aimed at modulating microbial communities to promote host health and mitigate disease states.

Methods

Bacterial Strains and Culturing Conditions

ID	Strain	Fluoresence	Abx Rx	Plasmid
BB121	*Aeromonas* sp. ZOR0001	dTOM	GentR	-
BB101	*Enterobacter* sp. ZOR0014	GFP	GentR, CamR	-
BB136	*Pleisomonas* sp.ZOR0011	dTOM	GentR	-
BB135	*Acinetobacter* sp.ZOR0008	dTOM	GentR	-
BB134	*Psuedomonas* sp.ZWU0006	dTOM	GentR	-
JS422	*E. coli* DH5a	-	GentR	pMQ72
BB106	*E. coli* DH5a	-	GentR	pMQ72::rcsDWT
BB104	*E. coli* DH5a	-	GentR	pMQ72::rcsDEV1
BB109	*Enterobacter* sp.ZOR0014	-	GentR, CamR	pMQ72
BB110	*Enterobacter* sp.ZOR0014	-	GentR, CamR	pMQ72::rcsDWT
BB111	Enterobacter sp.ZOR0014	-	GentR, CamR	pMQ72::rcsDEV1

All bacterial strains used in these studies were grown overnight at 30˚C with shaking in 5 ml Lysogeny Broth (LB) medium (10 g tryptone, 5 g yeast extract, and 10 g NaCl in 1000 ml of deionized) in the presence of antibiotic (10 µg/mL gentamycin and 25 µg/mL chloramphenicol) when indicated. All strains and samples from each passage in the experimental evolution were cryopreserved in equal volumes of 50% glycerol (25% final concentration) and stored at -80˚C.

Coaggregation Assay

Bacterial strains were cultured overnight as described in "*Bacterial Strains and Culturing Conditions"*. Overnight cultures then were washed, in sterile minimal medium (prepared stock solution concentrations are 5.03 mM NaCl, 0.17 mM KCl, 0.33 mM CaCl2•2H2O, 0.33 mM MgSO4•7H2O, and 0.1% (w/v) methylene blue) to remove the LB medium and products produced during overnight growth by centrifuging at 10,000 rpm for 2 minutes. The supernatant was removed, and the bacterial cell pellets were resuspended in sterile minimal medium and pelleted again. This was repeated two times.

Aggregation medium (250 µL) was added to each well, along with 150 µl of each washed bacterium. Aggregation medium is the minimal medium supplemented with 0.4% N-acetylglucosamine (GlcNac). The plates were then incubated with gentle shaking (120 RMP) for 6 hours at 30˚C. Coaggregation was quantified as described in the "*Quantification of Fluorescence*" section below.

Quantification of Coaggregation using Fluorescence Spectrometry

Following the incubation period in the coaggregation assay, a 150 µl sample of the planktonic (non-coaggregated) fraction was taken. The coaggregates were then gently resuspended using pipetting and another 150 µl sample taken representing the total bacteria in the well. Samples were taken in triplicate and transferred to black plastic glass bottom 96-well plates (Cellvis #P12-.15H-N). Fluorescence was measured using a Fluostar Omega BMG Labtech microplate spectrophotometer using the 485/520 and 544/590 (excitation/emission) to measure GFP and dTOM signals respectively. The fluorescence in each sample corresponds to the number of bacteria present in that sample and thus the formula *(total-planktonic)/total* applied to the GFP and dTOM values gives the fraction of aggregated GFP and dTOM labeled bacteria. Here, a value of 0 indicates little to no coaggregation while a value of 1 indicates virtually all the bacteria in the sample were aggregated.

Experimental Evolution

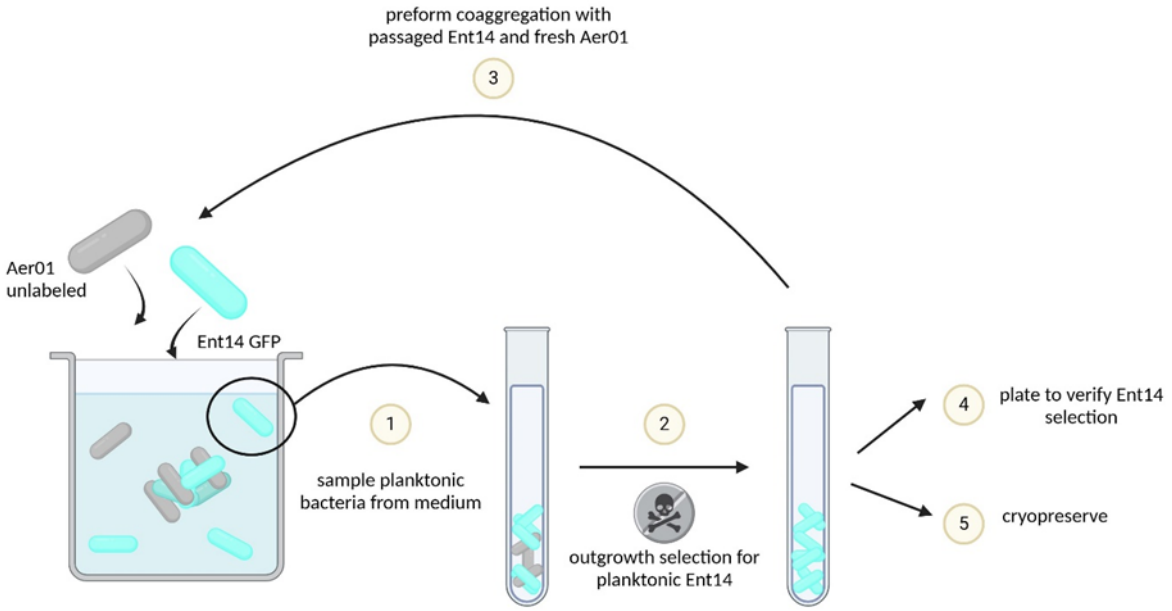

Figure 1: Experimental evolution to generate Enterobacter mutants that no longer coaggregate.

To generate *Enterobacter* mutants with defects in coaggregation with *Aeromonas*, I used a similar experimental design as detailed above in the "Coaggregation Assay", with slight modifications to serially passage and select non-coaggregating *Enterobacter*. Here, *Enterobacter*-GFP and unlabeled *Aeromonas* were used. After performing the initial coaggregation assay, a small portion (200 µl) of the non-aggregated bacterial population consisting of *Enterobacter* and *Aeromonas* cells, was sampled and inoculated into 5 mL of LB + 10 µg/mL gentamycin and 25 µg/mL chloramphenicol. *Enterobacter* is natively resistant to chloramphenicol while *Aeromonas* is sensitive, allowing enrichment of only *Enterobacter* from the non-aggregated sample. The enriched non-coaggregating *Enterobacter* were passaged into the next round of coaggregation with fresh unlabeled *Aeromonas*. Additionally, this *Enterobacter* outgrowth passage was cryopreserved for future analysis as well as plated on LB to verify no carryover of *Aeromonas*. This was repeated for a total of seven passages. *Enterobacter*

coaggregation in that passage was quantified as detailed in the "Quantification of Fluorescence" section above. This process was repeated for 7 passages, in which nearly no *Enterobacter* signal was detected in the *Aeromonas* aggregate.

Isolation of Enterobacter Mutants

A sample from each passage was plated on LB agar plates so that approximately 100-200 colonies grew per plate. I noted the emergence of mucoid colonies by the 3rd passage. Individual colonies were picked and grown in LB supplemented with Gent. We randomly selected 2 mucoid colonies and 1 colony with wild-type colony morphology. Isolated *Enterobacter* mutants were assayed for coaggregation defects.

Fluorescence Confocal Microscopy

The indicated strains were cocultured in black 12-well glass bottom plates (Cellvis #P12-.15H-N) following the aggregation assay protocol. After the 6-hr. incubation period, approximately half of the liquid volume (1 mL) was discarded to allow aggregates to contact the glass bottom surface for live imaging of the aggregate structures.

Microscopy images were acquired on a Nikon CSU-W1 SoRa Spinning Disk equipped with a Prime BSI sCMOS camera, with 488 nm and 561 nm excitation lines, and a 60X water immersion objective. Acquisition was performed using Nikon Elements. False coloring was done using the software FIJI.

Genomic Analysis of Evolved Mucoid Enterobacter

The genomic DNA of WT, EV1, and EV3 were purified using the QIAGEN DNeasy Blood and Tissue Kit (Cat# 69504) according to the manufactures protocol. Genome sequencing, assembly, and annotation were performed by Plasmidsaurus (https://www.plasmidsaurus.com/).

Long-read sequencing technology from Oxford Nanopore Technologies was used for genome sequencing. Genomes were assembled using and annotated using Plasmidsaurus' pipeline outlined at https://www.plasmidsaurus.com/faq/#bact-assembly. Mutations present in EV1 and EV3 were identified using *breseq* using default parameters and the EV1 or EV3 fastq files against the WT assembled reference genome.

Sedimentation Resistance Assay

Sedimentation resistance was used to assay Rcs activation as described previously (Kessler 2021) Bacteria were cultured overnight in 5 mL of LB supplemented with or without 0.4% glucose and 10 µg/mL gentamycin. A 1.5 mL sample was aliquoted into a 1.5 mL centrifuge tube and centrifuged at 10,000 rpm for 2 minutes to induce sedimentation. After centrifugation, sedimentation resistance was observed by visually inspecting the turbidity of the supernatant. An increase in turbidity indicated an increase in sedimentation resistance and thus increased Rcs activity. To quantify sedimentation resistance, samples were first normalized to an OD_{600} of 1.0 and then centrifuged 10,000 rpm for 2 min. 150 µl samples of the supernatant were then added to a black plastic glass bottom 96-well plates (Cellvis #P12-.15H-N). The OD_{600} was measured in the Omega BMG Labtech microplate spectrophotometer.

Construction of $RcsD^{WT}$ and $RcsD^{EV1}$ Expression Plasmids

The expression plasmid pMQ72 was first linearized using the restriction enzyme SmaI.

Next, the *rcsD* region WT *Enterobacter* or the EV1 isolated was amplified using primers JP203(5'GGGCTAGCGAATTCGAGCTCGGTACCCtttgtTTAACTTTAagAAGGAGatataCATatgagtcagactgaaac taccg-3') and JP204(5'-AAGCTTGCATGCCTGCAGGTCGACTCTAGAGGATCCCCctacagcaagcttttgacgtag-3'). The PCR products were resolved using gel electrophoresis and the bands corresponding to

the predicted PCR produce size were excised using a gel extraction tool and purified using the Zymo Gel Extraction kit.

The WT or EV1 *rcsD* amplicons were each combined with SmaI cut pMQ72 and then mixed with equal parts of 2X Gibson Assembly Master Mix (#E2611L) The assembly reaction was incubated at 50˚C for 45 minutes. The plasmid assembly mixture (5 µl) was added transformed into high efficiency chemically competent DH5a *E. coli* purchased from NEB (#C2987H) Briefly, a tube of NEB 5-alpha Competent *E. coli* cells was thawed on ice for 10 minutes. Subsequently, 5µl of the Gibson assembly reaction was added to the cell mixture and placed on ice for 30. The cells were then heat shocked at 42°C for 30 seconds, then returned to ice for 5 minutes. Next, 950 µl of room temperature SOC was pipetted into the mixture, and the solution was incubated at 37°C for 60 minutes with vigorous rotation. Cells were plated on LB agar plates containing 10 µg/mL Gent and incubated at 30˚C for 24 hrs.

To verify insertion of each rcsD allele, colony PCR was performed using primers JP09 (5'- gcacggcgtcacactttgctatgccatag-3') and JP10 (5'- gcgctacggcgtttcacttctgagttcg-3') that anneal on pMQ72 just outside of where the *rcsD* allele is inserted. In this reaction, colonies carrying plasmid with the *rcsD* gene integrated would produce a 2.7 kb amplicon while empty vector would produce a 350 bp amplicon. Gel electrophoresis was used to resolve the PCR bands.

Three colonies were selected from each transformation and cryopreserved. Plasmid was miniprepped from each strain using the QIAGEN Miniprep Kit (# 27104) and subsequently sequenced by Plasmidsaurus. Miniprepped plasmid carrying the correct sequence as verified by Plasmidsaurus sequencing was then transformed into electrocompetent *Enterobacter*.

Preparation of Electrocompetent Enterobacter

Enterobacter were grown overnight in LB and 100µl of overnight growth was plated onto LB agar plate. The LB agar plate was incubated at 37˚C for 5 hrs and Enterobacter growth was scraped from the plates using sterile technique into 1 mL ice cold water. This cell mixture was pelleted for 5 min at 5k x g at 4˚C and the supernatant discarded. Cells were similarly washed two more times in 1 mL ice cold water. The cell pellet was finally resuspended into 150µl ice cold water and 50 µl aliquoted into 3 microcentrifuge tubes. Approximately 100 ng of pMQ72, pMQ72::rcsD^{WT}, or pMQ72::rcdD^{EV1} was added to the respective tubes then transferred to pre-chilled 1 mm cuvettes. Enterobacter was then electroporated in a 1mm cuvette at 1.8 kV. Cells recovered in 1 ml of LB for one hour at 37 C then plated on plates and incubated overnight at 37 C. Three colonies per transformation were cultured in 5 mL LB/Gent and cryopreserved.

Results

Aer01 and Ent14 Coaggregate in Culture

To measure Aer01 and Ent14 coaggregation, I used culture conditions previously shown to stimulate Aer01 aggregation (Smith 2023). Using the coaggregation assay with Aer01 constitutively expressing the red fluorophore dTomato (Aer01-dTom) and Ent14 constitutively expressing green fluorescent protein (Ent14-GFP), I found macroscopic aggregates were formed within 6 hours of coculture in Aer01 containing wells, whereas Ent14 alone does not form macroscopic aggregates (Fig. 2A). Aer01-dTOM and Ent14-GFP aggregation was quantified using fluorescence spectrometry by reading the dTOM and GFP values in each sample before (planktonic cells) and after the aggregate structures were manually resuspended into single cells (total cells). Using the equation (total cells-planktonic cells)/total cells on the dTOM and GFP values yielded the fraction of aggregated cells in each fluorescence channel, indicating Aer01-dTOM and Ent14-GFP are aggregated at this time point (Fig. 2B).

To determine if these aggregates were distinct aggregates of Ent14-GFP or Aer01-dTOM, or coaggregates of these two species, I used confocal fluorescence microscopy on live cells, which allowed for high resolution of the aggregates without disrupting their structural features. I found that Aer01-dTom and Ent14-GFP were organized in mixed coaggregates (Fig. 2C).

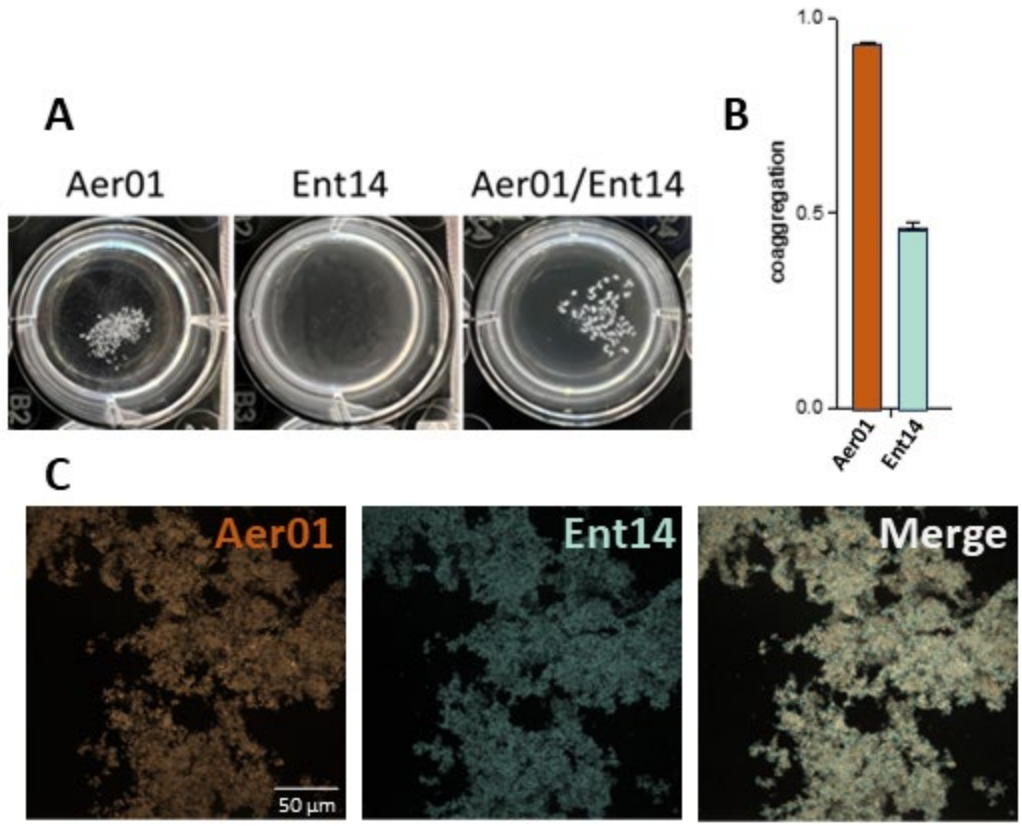

Figure 2: Aer01-dTom and Ent14-GFP coaggregate in coculture. (A) Macroscopic aggregates formed within 6 hours of coculture are visible by eye. (B) Quantification of Aer01-dTom and Ent14-GFP aggregation using fluorescence spectrometry, indicating the fraction of aggregated cells at this time point. (C) Confocal fluorescence microscopy confirms the presence of coaggregated Aer01-dTom and Ent14-GFP within macroscopic aggregates. (scale bar is 50µm. All images were acquired at the same magnification)

An Aer01 Adhesin Facilitates Coaggregation with Ent14

To dissect the molecular basis of coaggregation between Aer01 and Ent14, I first focused on Aer01 factors that might facilitate coaggregation. I leveraged an Aer01 mutant, MB1, which lacks a functional mucin-regulated adhesin called MbpA and does not aggregate under our culture conditions (Smith, 2023). I posited this mutant might reveal the directionality of coaggregation of Aer01 and Ent14. I hypothesized that the Aer01 MbpA adhesin facilitates coaggregation by binding a shared cell surface feature in both Aer01 and Ent14.

To test this idea, I first determined if MB1 could coaggregate with wild-type Aer01. If MbpA drives Aer01 aggregation by binding MbpA on the surface of neighboring cells, I would

expect the MB1 mutant to be excluded from Aer01 aggregates in coaggregation assay. However, using confocal fluorescence microscopy, I found MB1-dTOM coaggregates with Aer01-GFP (Fig. 3A), indicating MbpA drives Aer01 aggregation by binding a cell surface feature other than MbpA. Surprisingly, MB1-dTOM did not coaggregate with Ent14-GFP, suggesting MbpA interactions with an unknown surface component on Ent14 are required for coaggregation between these species (Fig 3B). Together these data suggest Aer01 uses MbpA to interact with other Aer01 cells as well as Ent14, likely by binding a cell surface feature shared among these different bacteria.

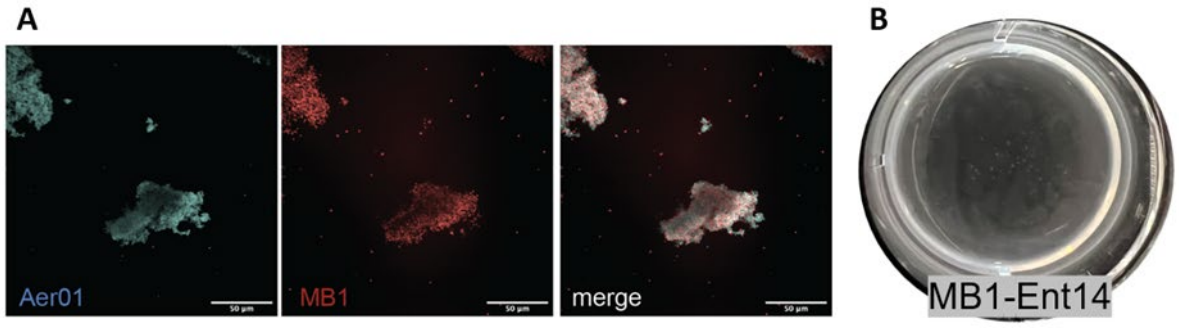

Figure 3: The Aer01 adhesin, MbpA, is required for Aer01-Ent14 coaggregation. (A) Confocal fluorescence microscopy reveals coaggregation of MB1-dTOM (*mbpA* mutant) with Aer01-GFP (wild-type). (B) MB1-dTOM does not coaggregate with Ent14-GFP.

Experimental Evolution Selects for Mucoid Enterobacter with Coaggregation Defects.

I next sought to identify the cell surface component that MbpA binds on Ent14. I leveraged the tight coaggregation observed between Aer01 and Ent14 in our coculture conditions to develop an experimental evolution regime to select for Ent14 with defects in coaggregation with Aer01. I reasoned that Ent14 with coaggregation defects will have mutations that result in a loss of the cell surface component recognized by MbpA. The experimental approach is outlined in Figure 1. Aer01 and Ent14-GFP were cocultured as previously in the coaggregation assay. A sample of non-coaggregating (planktonic) bacteria was obtained by sampling the media outside

of the coaggregate after it had formed. This planktonic sample was cultured overnight in rich growth medium under conditions that allow only growth of Ent14-GFP. This passaged Ent14-GFP was added to coaggregation assay with fresh Aer01. I used Ent14-GFP to track Ent14 coaggregation at each passage step. Within seven passages, I observed a significant reduction in Ent14-GFP coaggregation in this evolved population (P7) compared to the parental strain (P0) (Fig. 4A).

At each passage I plated the overnight growth to ensure I selected against Aer01 growth. By the third passage I noted the emergence of mucoid Ent14-GFP isolates that dominated the population by the seventh passage (Fig. 4B, note arrows). This observation corresponded with a significant drop of coaggregated Ent14-GFP by the seventh passage. The parental Ent14-GFP typically forms relatively small colonies, while the mucoid isolates are shiny and orders of magnitude larger. Importantly, Aer01 aggregated throughout experimental evolution, indicating changes in Ent14's ability to coaggregate with Aer01 did not impact Aer01 aggregation.

To determine if the mucoid isolates display defects in coaggregation with Aer01, I selected two mucoid colonies and one colony with a colony morphology indistinguishable from parental Ent14. Mucoid isolates demonstrated a significant decrease in coaggregation as indicated by fluorescence spectrometry, while isolates with the wild-type colony phenotype exhibited coaggregation behavior similar to the ancestral Ent14-GFP (Fig. 4C). Confocal fluorescence microscopy verified the two mucoid isolates were poorly coaggregated with Aer01-dTOM (Fig. 4D) and more planktonic, existing mostly as single cells. These two mucoid Ent14 isolates were renamed EV1 and EV3 and were further characterized.

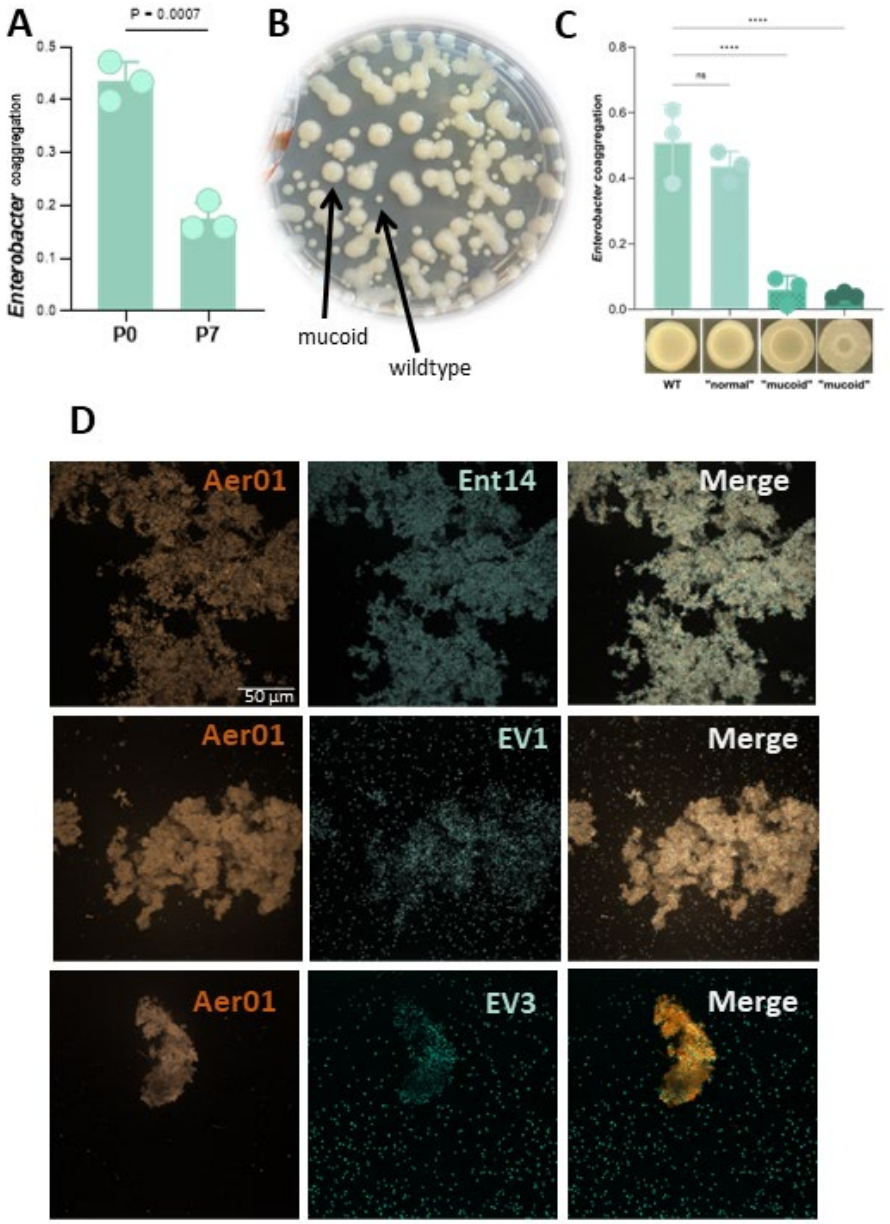

Figure 4: Characterization of Ent14-GFP isolates generated through experimental evolution. (A) Coaggregation of the parental Ent14-GFP and evolved population after seven passages. (B) The mucoid colony morphology dominates the Ent14-GFP evolved population by the seventh passage. (C) Quantification of coaggregation for mucoid isolates compared to isolates with wild-type colony morphology. (D) Confocal fluorescence microscopy of mucoid isolates (EV1 and EV3) with Aer01-dTOM. Note planktonic Ent14 not observed in Figure 1D. (scale bar is 50µm. All images were acquired at the same magnification)

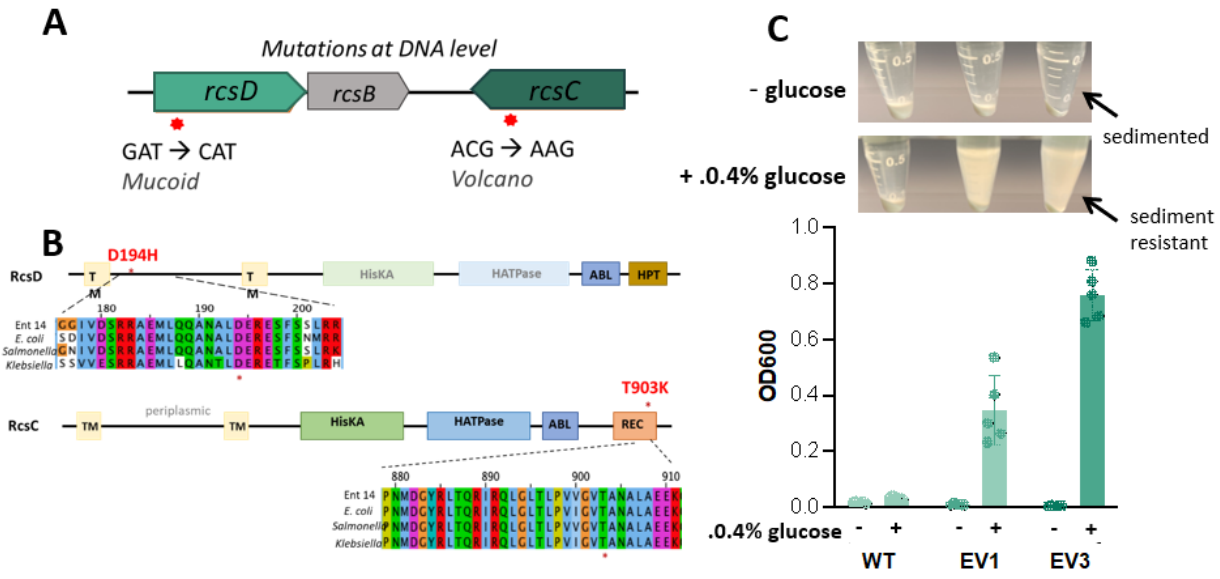

Figure 5: Mucoid Ent14 have mutations in the Rcs system. (A) Genetic mutations identified in EV1 and EV3. (B) Non-synonymous mutations in RcsD and RcsC genes of EV1 and EV3, resulting in residues D194H and T903K, respectively. RcsC and RcsD are highly similar among Enterobacteriaceae. (C) EV1 and EV3 exhibit sedimentation resistance in Rcs-stimulating conditions, a hallmark of hyperactive Rcs signaling.

EV1 and EV3 Have Mutations in the Rcs Pathway.

To investigate the genetic basis of the mucoid phenotype in my EV1 and EV3 isolates, I isolated and sequenced their genomes, then identified nucleotide changes in the genomes of these mutants by comparing these genomes to the ancestral Ent14-GFP genome using the software *breseq*. My analysis uncovered two independent mutations in genes belonging to the same signaling pathway. I found that EV1 has a **G**AT→**C**AT mutation in the *rcsD* gene while EV3 has an A**C**G→A**A**G mutation in the *rcsC* gene (Fig. 5A).

Rcs signaling has been shown to control mucoidy in *Enterobacteriaceae,* to which Ent14 belongs, by modulating production of long sugar polymers called extracellular polysaccharides such as colanic acid polysaccharide (CAP). The genomic changes I identified in EV1 and EV3 both generate non-synonymous mutations. In EV1 the change corresponded to residues D194H

in periplasmic region of RcsD. In EV3 the change corresponded to T903K in the C-terminal region of RcsC (Fig. 5B). Consistent with our findings, previous studies in *Salmonella* identified a T903A mutation in RcsC that conferred mucoidy (García-Calderón, 2005), suggesting this residue is important for controlling the mucoid phenotype in distantly related bacterial genera. The periplasmic region of RcsD has been shown to interact with IgaA, which suppresses Rcs activation (Rodriguez, 2023), suggesting the RcsD D194H allows hyperactive Rcs signaling under some conditions by decreasing typical interactions with IgaA. Mucoidy is a known phenotype caused by hyperactive Rcs signaling, which is highly conserved in *Enterobacteriaceae* (Fig 5B, alignment).

Mucoid Enterobacter Are Hyperactive CAP Producers

Previous studies found that mucoid *E. coli* with hyperactive Rcs activity produces more colanic acid polysaccharide (CAP) and are more resistant to sedimentation when grown in Rcs-stimulating conditions such as LB supplemented with 0.4% glucose (Kessler, 2021). Unlike wild-type *E. coli*, hyperactive Rcs mutants show resistance to centrifugation resulting in a more turbid supernatant. This turbidity, or sedimentation resistance, can be measured by reading optical density at 600 nm (OD600) after centrifugation. Thus, elevated OD600 values indicate increased sedimentation resistance and increased Rcs activity under a given condition. Previous data suggest that the sedimentation resistance phenotype is correlated with how much CAP remains attached or is shed from the cell surface (Kessler, 2021).

To test if EV1 and EV3 have hyperactive Rcs signaling, we grew these strains and ancestral Ent14 in LB medium with or without 0.4% glucose. EV1 and EV3 demonstrated sedimentation resistance in glucose-rich conditions only and the ancestral Ent14 did not resist

sedimentation in either condition (Fig. 5C). These results are consistent with the idea that EV1 and EV3 mutations render the Rcs system hyperactive under certain conditions and suggest that the mucoidy observed in the evolved isolates is related to Rcs system activity.

The rcsD^{EV1} Allele is Sufficient to Cause Mucoidy in the Parental Ent14

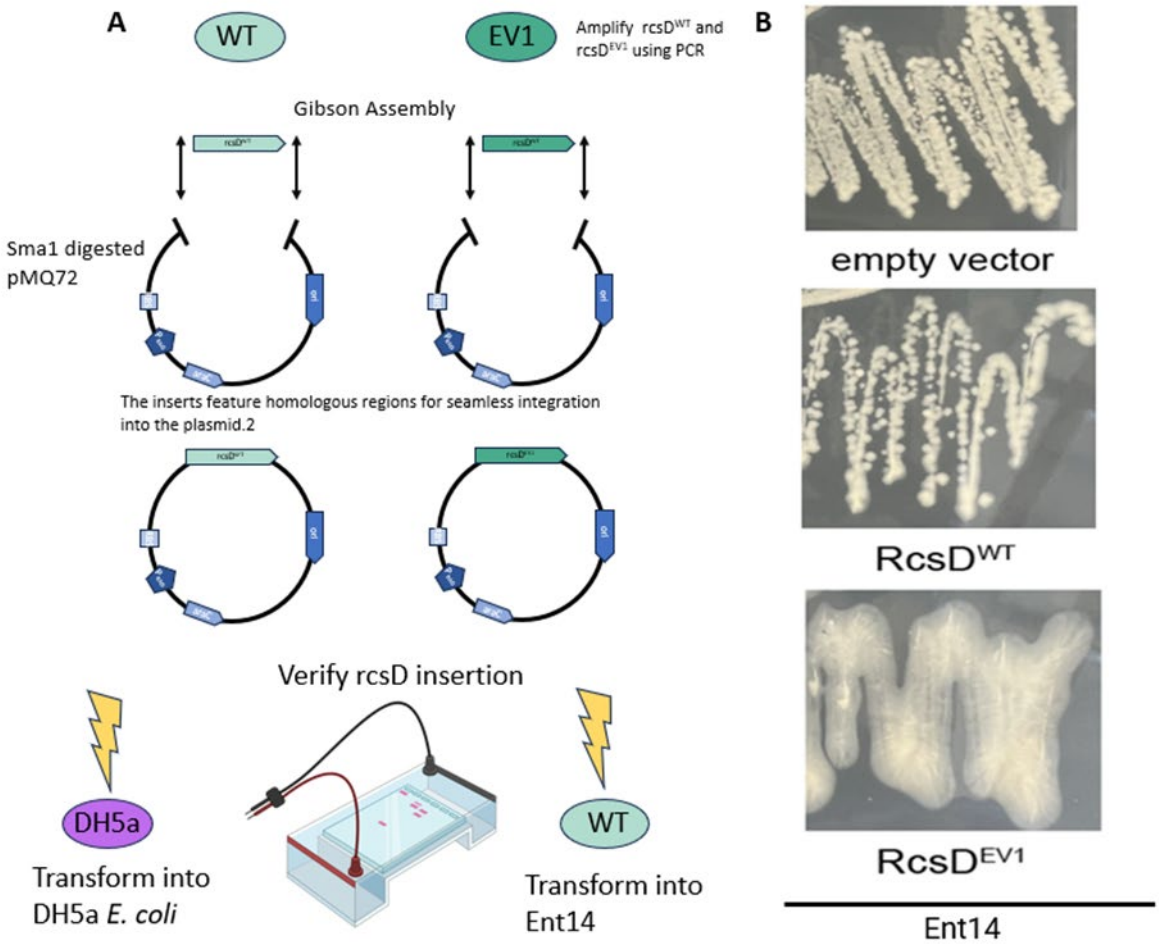

Figure 6: The EV1 *rcsD* allele is sufficient to cause mucoidy in wild type Ent14. (A) Schematic representation of the plasmid-based strategy for introducing either wild-type (*rcsD^{WT}*) or mutated (*rcsD^{EV1}*) *rcsD* gene into Ent14. (B) Mucoidy assessment on LB agar plates showing the absence of mucoid phenotype in RcsD^{WT} Ent14 and the presence of mucoid phenotype in RcsD^{EV1} Ent14.

Mutations in *rcsD* have been shown to induce mucoidy despite the presence of the wild-type allele (Kessler, 2021). To determine whether the EV1 mutation in *rcsD* (*rcsD^{EV1}*) is

sufficient to cause mucoidy in wild-type Ent14, we cloned the wild type and EV1 rcsD alleles into the expression plasmid pMQ72 and transformed these constructs into wild type Ent14 (Fig 6A).

Next, I compared the colony morphology of Ent14 carrying pMQ72 (empty vector), pMQ72::rcsD^{WT} (RcsD^{WT}), or pMQ72::rcsD^{EV1} (RcsD^{EV1}) to assay for mucoidy. Together, these data indicate the RcsD^{EV1} mutation is sufficient to cause mucoidy, and that expressing higher levels of wild-type RcsD itself does not impact Ent14 colony morphology under these conditions (Figure 6B).

Mucoid Enterobacter Disrupt Aggregate Structures of Resident Microbes

While I focused my initial studies on how Ent14 interacts with Aer01, various genera of bacteria reside in the larval zebrafish gut and likely have the opportunity to physically interact with Ent14. To determine the extent to which hyperactive Rcs signaling might impact potential interactions with Ent14 and other resident microbes of the larval zebrafish gut, I assayed coaggregation between Ent14-GFP or EV1 and three diverse bacterial isolates from our larval zebrafish collection using confocal fluorescence microscopy. The isolates chosen were *Pseudomonas* ZWU0006 (Pse06), *Pleisomonas* ZOR0011 (Ple11), and *Acinetobacter* ZOR0008 (Ac08). As with Aer01, each of these isolates were previously engineered to constitutively express dTOM (Wiles, 2018).

I found Ent14 forms micro-coaggregates with Pse06, Ac08, and Ple11 (Fig. 7A). Coaggregates with Ple11 are well mixed while coaggregates with Pse06 and Ac08 were less compact, containing many small aggregates but also planktonic cells. When cocultured with EV1, the three bacterial strains each exhibited a near total loss of aggregate or coaggregate formation (Fig. 7B). This observation was surprising as Pse06, Ac08, and Ple11 form

microaggregate structures when grown alone under these conditions (Fig. 7C). This observation contrasts with what we observed with Aer01, whose aggregation was not impacted by the presence of EV1. Collectively, these data demonstrate that mucoidy interferes not only with the formation of coaggregate communities but also can impact typical aggregation and physiological traits of other bacteria in the community.

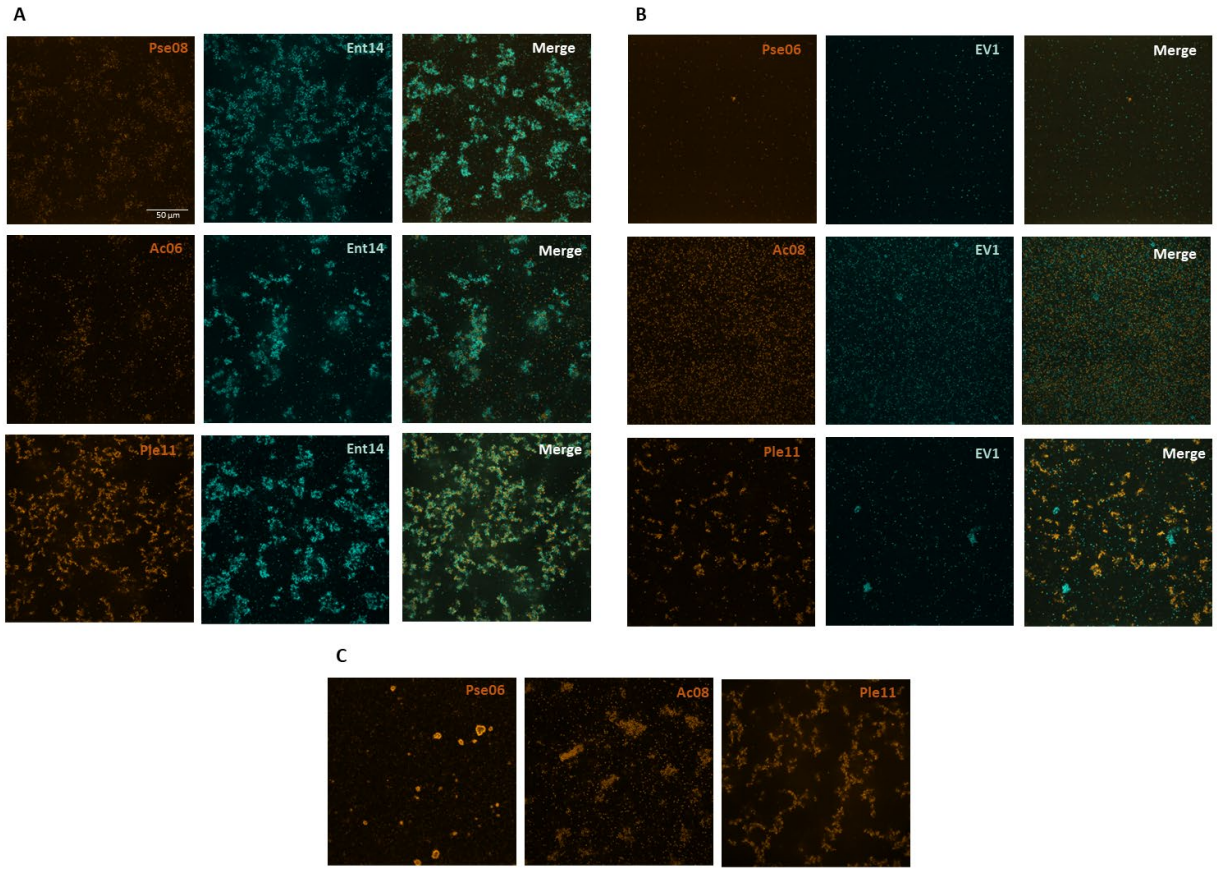

Figure 7: Impact of mucoid EV1 isolate on coaggregation with diverse bacterial isolates from larval zebrafish gut. (A) Confocal fluorescence microscopy showing micro-coaggregates formed between Ent14 and Pse06, Ac08, and Ple11 (B) Coculture of mucoid EV1 (teal) with diverse bacterial isolates results in suppression of aggregation of Pse06 and Ac08, with only small clusters of Ple11 observed in the presence of EV1. (C) monoculture of Pse06, Ac08, and Ple11 showing microaggregate formation. (scale bar is 50µm. All images were acquired at the same magnification)

Discussion

The assembly of microbial communities is a fundamental process in ecology, shaping the structure and function of ecosystems across diverse habitats. Within these communities, bacteria engage in complex physical and chemical interactions, forming aggregates that serve as hubs for cooperation, competition, and nutrient exchange. Coaggregation, the adherence of multiple bacterial species to one another, drives the physical assembly of microbial communities in virtually every environment, from geothermal vents to the intestines of humans. However, we still have a poor molecular understanding of how and why microbial communities assemble.

In my thesis studies, I uncovered the molecular basis of coaggregation between two resident microbes of the larval zebrafish gut, Aer01 and Ent14. I found Aer01 uses a large adhesin with multiple glycan-binding repeats called MbpA, to bind a yet known factor on cell surface of Ent14. To identify this factor, I used an innovative experimental evolution approach to enrich for Ent14 mutants with coaggregation defects with Aer01. I was able to rapidly generate Ent14 isolates with impaired coaggregation and identified the genetic basis for these defects. I observed the emergence of mucoid Ent14 isolates early into the experimental evolution and found mucoidy Ent14 have significant coaggregation defects when cocultured with Aer01. I expanded my studies to determine how Ent14 mucoidy impacts interactions with other resident microbes of the larval zebrafish gut, namely Pse06, Ac08, and Ple11. Mucoid Ent14 exhibited coaggregation defects with Pse06, Ac08, and Ple11. These defects show the suppression of aggregation of these species by mucoid Ent14. This is in stark contrast to Aer01, which aggregates in the presence of mucoid Ent14, but does not bind this mutant. These unexpected results highlight the dramatic impact the physiology of one microbe can have on community organization and point to potential rules for community assembly and disruption.

Mucoidy refers to a bacterial phenotype characterized by the production of protective cell surface associated substances like exopolysaccharides. Mucoidy often arises when bacteria encounter environmental stressors such as bacterial-targeting toxins, host immune cells, or bacteriophage that target cell surface factors such as outer membrane efflux pumps that are essential for bacterial survival (Akoolo, 2022; Hsieh, 2020; Raus-Madiedo, 2009). Under chronic pressure, bacteria adopt a mucoid phenotype to protect these indispensable components, despite the energetic costs. The mutations I found highlight Rcs as the molecular basis for the mucoid phenotype. The rapid emergence of mucoid Ent14 suggests MbpA binds a cell surface factor that is critical for Ent14 survival in our coculture conditions. This idea is supported by the observation that the extracellular portion of MbpA contains repeated protein domains similar to bacteriophage receptor binding proteins. While the specific identity of this factor remains unknown, my research provides valuable insights into the role of Rcs signaling in mediating microbe-microbe interactions. Future studies could use a similar experimental evolution approach with a mutant of *Enterobacter* mutant that cannot convert to mucoidy to select for loss of the MbpA target without selecting for mucoid conversion.

The Rcs system is known to control mucoidy in Enterobacteriaceae, the family to which Ent14 belongs. High sequence similarity of this system among diverse strains points to the strong selective pressure for bacteria to conserve this pathway for responding to common environmental stressors (Meng, 2021). RcsC and RcsD function as inner membrane-bound sensor kinases, regulating the levels of phosphorylated RcsB to adapt to environmental stressors (Clarke, 2010). RcsC can function as a kinase that phosphorylates RcsD to activate Rcs signaling or a phosphatase that de-phosphorylates RcsD to decrease Rcs signaling. Recent studies (Wall, 2020) revealed inhibitory interactions between RcsD and IgaA that take place within the periplasmic

domains of both proteins, which also repress RcsD-RcsC signaling to RcsB, but the amino acid residues involved in this interaction are unknown. Thus, a *rcsD* mutation that decreases RcsD-IgaA interactions would increase Rcs signaling and promote mucoidy. The mutation in RcsD of D194H that I recovered in the EV1 evolved isolate, is located in the periplasmic region. Since IgaA-binding inhibits RcsD signaling, my data suggests D194 may be a critical residue in the interaction interface between RcsD and IgaA and regulation of CAP biosynthesis. This aspartic acid residue is conserved in Rcs systems in Enterobacteriaceae, suggesting a critical role among diverse Rcs-encoding microbes.

Mucoid conversion can decrease or increase the virulence potential of microbes depending on the environmental context and genetic capacity of the microbe being studied. In *Salmonella enterica*, a *rcsC* similar to the mutation seen in my EV3 reduces its virulence in mouse models, while in *Pseudomonas aeruginosa*, mucoidy is associated with chronic infections and worse clinical outcomes. This highlights the dynamic effects of mucoidy across bacteria species and the need to better understand the impact of mucoid on physical and chemical interactions with other microbes.

While CAP and other capsule polysaccharide are cell surface associated, a fraction are also shed into the environment, which could serve as a sugar-rich chemical cue to nearby microbes (Kessler, 2021). Supernatants from EV1 and EV3 mutants exposed to Rcs-activating media were more turbid than wildtype, indicating increased CAP shedding. Observations of the pairwise interactions between Ent14 and other zebrafish gut isolates provide crucial insights into how the physical and chemical traits of CAP can shape microbial physiology and impact microbial ecology. For instance, when EV1 is paired with Aer01, Aer01 maintains its aggregate structure, suggesting that CAP attached to EV1 blocks MbpA binding to EV1 but does not

impact MbpA's function in Aer01 aggregation. However, when EV1 is paired with other Pse06, Ac08, or Ple11, it completely disrupts and inhibits their aggregation, which in turn inhibits coaggregation.

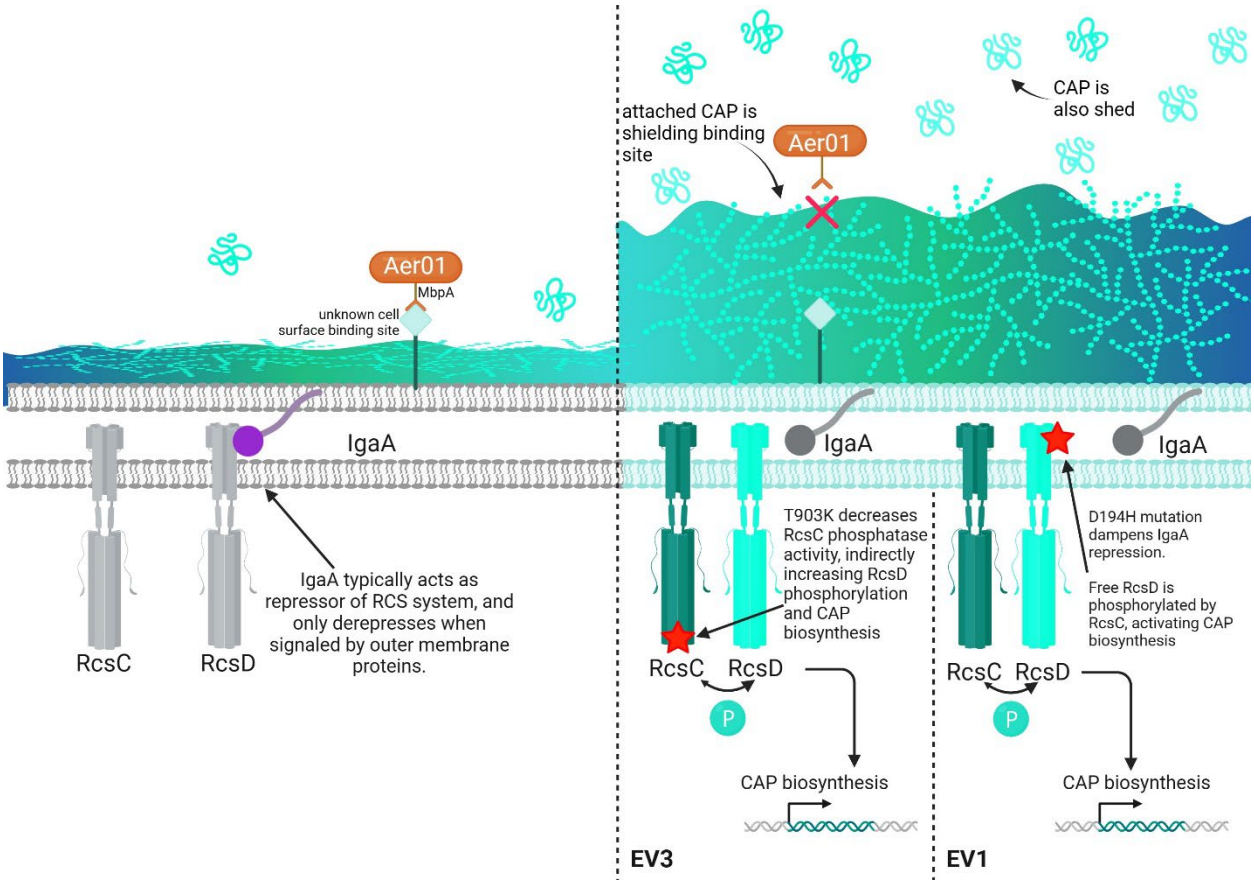

Figure 8: Schematic model of Rcs signaling in wildtype Ent14 compared to EV1 and EV3 mucoid isolates. This diagram demonstrates potential scenarios for each where CAP biosynthesis is being upregulated.

By considering the intricate relationship between mucoidy, coaggregation, and bacterial physiology, this study opens promising avenues for future research in microbial ecology and host-microbe interactions. One intriguing area for further investigation is the impact of mucoidy on broader community dynamics within the gut microbiome. Exploring how the physiological state of one microbe, such as mucoidy, influences the behavior and function of other members of the community could provide valuable insights into the mechanisms driving community assembly and stability. Additionally, deeper investigation into the regulatory pathways

underlying mucoidy, such as the Rcs-mediated upregulation of capsule production, offers opportunities to uncover novel therapeutic targets for manipulating microbial communities to promote host health. Furthermore, investigating the ecological consequences of mucoidy conferred by CAP overproduction may shed light on how microbial traits shape ecosystem processes and resilience.

These discoveries provide new molecular insights into the mechanisms by which host-associated bacteria organize themselves into co-aggregates within the gut environment. Specifically, the increased shedding of CAP by certain bacterial mutants can disrupt the aggregation of some bacterial species while preserving the structures of others. This differential impact on microbial aggregation reveals how physical and chemical traits of CAP influence microbial physiology and interactions. Additionally, the phenomenon of mucoidy suggests a mechanism by which bacteria might evade coaggregation with other bacteria, potentially as a strategy to avoid unfavorable interactions. Understanding these dynamics is crucial for comprehending how bacterial community membership shapes host health, as disruptions in aggregation and community balance can impact gut health and disease states. Overall, continued research in this field promises to deepen our understanding of microbial community ecology and its implications for host health.

Bibliography

Akoolo, L., Pires, S., Kim, J., & Parker, D. (2022). The capsule of Acinetobacter baumannii protects against the innate immune response. *Journal of innate immunity*, 14(5), 543–554. https://doi.org/10.1159%2F000522232

Anselmi, G., Gagliardi, L., Egidi, G., Leone, S., Gasbarrini, A., Miggiano, G. A., & Galiuto, L. (2020). Gut microbiota and cardiovascular diseases. Cardiology in Review, 29(4), 195–204. https://doi.org/10.1097/crd.0000000000000327

Bates JM, Mittge E, Kuhlman J, Baden KN, Cheesman SE, Guillemin K. (2006). Distinct signals from the microbiota promote different aspects of zebrafish gut differentiation. *Dev Biol*, 297(2), 374-86. https://doi.org/10.1016/j.ydbio.2006.05.006

Breton, J., Galmiche, M., & Déchelotte, P. (2022). Dysbiotic gut bacteria in obesity: An overview of the metabolic mechanisms and therapeutic perspectives of next-generation probiotics. Microorganisms, 10(2), 452. https://doi.org/10.3390/microorganisms10020452

Bunyavanich, S., & Berin, M. C. (2019). Food allergy and the microbiome: Current understandings and future directions. Journal of Allergy and Clinical Immunology, 144(6), 1468–1477. https://doi.org/10.1016/j.jaci.2019.10.019

Fung TC, Artis D, Sonnenberg GF. Anatomical localization of commensal bacteria in immune cell homeostasis and disease. (2014). *Immunol Rev*, 260(1), 35-49. https://doi.org/10.1111/imr.12186

García-Calderón, C. B., García-Quintanilla, M., Casadesús, J., & Ramos-Morales, F. (2005). Virulence attenuation in salmonella enterica RCSC mutants with constitutive activation of the RCS System. *Microbiology*, 151(2), 579-588. https://doi.org/10.1099/mic.0.27520-0

Hsieh, S. A., & Allen, P. M. (2020). Immunomodulatory roles of polysaccharide capsules in the intestine. *Frontiers in immunology*. 11, 690. 11:690. https://doi.org/10.3389/fimmu.2020.00690.

Kennedy, P. J. (2014). Irritable bowel syndrome: A microbiome-gut-brain axis disorder? World Journal of Gastroenterology, 20(39), 14105. https://doi.org/10.3748/wjg.v20.i39.14105

Kessler, N. G., Caraballo Delgado, D. M., Shah, N. K., Dickinson, J. A., & Moore, S. D. (2021). Exopolysaccharide anchoring creates an extreme resistance to sedimentation. *Journal of bacteriology*, 203(11), 1-19 https://doi.org/10.1128/jb.00023-21

Levy, M., Kolodziejczyk, A., Thaiss, C., & Elinav, E. (2017). Dysbiosis and the immune system. *Nature reviews Immunology* 17(4):219-232. https://doi.org/10.1038/nri.2017.7.

Meng, J., Young, G., & Chen, J. (2021). The RCS system in Enterobacteriaceae: Envelope stress responses and virulence regulation. *Frontiers Microbiology*, 12. https://doi.org/10.3389/fmicb.2021.627104

Metchnikoff, E. (1908). The Prolongation of Life. Nature News. https://www.nature.com/articles/077289b0

Rodriguez, L., Penalver, M., Casino, P., & Portillo, F. G. D. (2023). Evolutionary analysis and structure modelling of the RCS-repressor IgaA unveil a functional role of two cytoplasmic small β-barrel (SBB) domains. *Heliyon*, 9(6):e16661. https://doi.org/10.1016/j.heliyon.2023.e16661

Ruas-Madiedo, P., Gueimonde, M., Arigoni, F., de los Reyes-Gavilán, C. G., & Margolles, A. (2009). Bile affects the synthesis of exopolysaccharides by Bifidobacterium animalis. *Applied and environmental microbiology*, 75(4): 1204–1207. https://doi.org/10.1128%2FAEM.00908-08

Smith, T. J., Sundarraman, D., Melancon, E., Desban, L., Parthasarathy, R., & Guillemin, K. (2023). A mucin-regulated adhesin determines the intestinal biogeography and inflammatory character of a bacterial symbiont. *Cell Host Microbe.* https://doi.org/10.1016/j.chom.2023.07.003.

Wiles, T., Wall, E. S., Schlomann, B. H., Hay, E. A., Pathasarathy, R., & Guillemin, K. (2018). Modernized tools for streamlined genetic manipulation and comparative study of wild and diverse proteobacterial lineages. *mBio*, 9(5): e01877-18. https://doi.org/10.1128%2FmBio.01877-18